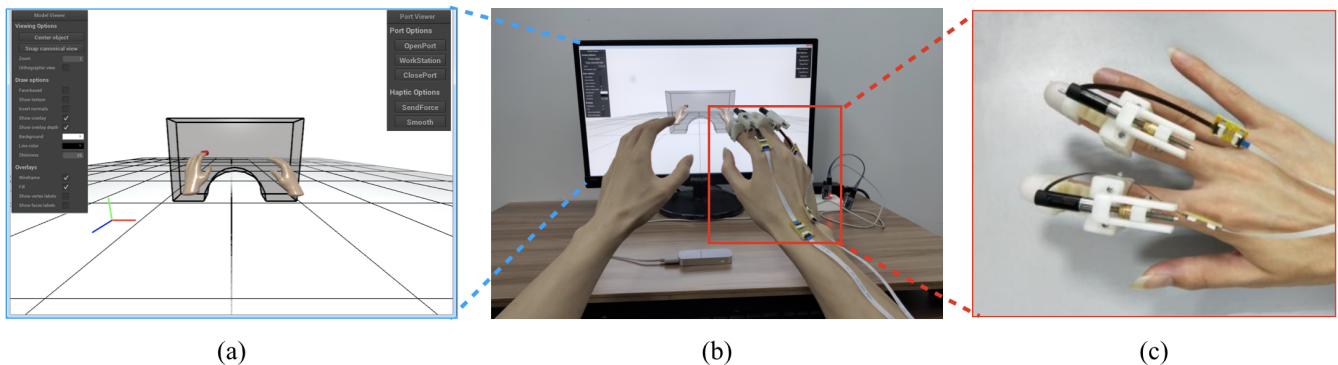


# Feel the Inside: A Haptic Interface for Navigating Stress Distribution Inside Objects



**Figure 1:** Navigating the stress distribution of a model under loads using our system.

## Abstract

Understanding stress distributions over 3D models is a highly desired feature in many scientific and engineering fields. The stress is mathematically a rank-2 tensor, and it is typically visualized using either color maps, tensor glyphs, or streamlines. However, neither of these methods is physically intuitive to the end user, and they become even more awkward when dealing with the volumetric tensor field over a complicated 3D shape. In this paper, we present a virtual perception system, which leverages a multi-finger haptic interface to help users intuitively perceive 3D stress fields. Our system allows the user to navigate the interior of the 3D model freely and maps the stress tensor to the haptic rendering along the direction of the finger's trajectory. Doing so provides user a natural and straightforward understanding of the stress distribution without interacting with the parameters in the graphics-based visual representations. Experimental results show that our system is preferred in navigating stress fields inside an object and is applicable for different design tasks.

## CCS Concepts

• **Computing methodologies** → Collision detection; • **Hardware** → Sensors and actuators; PCB design and layout;

## 1. Introduction

Stress is a physics quantity in continuum mechanics, which expresses the internal forces that neighboring particles of a continuous material exert on each other. Stress field of an object varies with its deformation under specified loads or constraints. The material is prone to fail at the places where the stress is higher. Therefore, it is a key index in structural analysis with various applications in material and shape modeling in industrial design [KSZ\*14], strength analysis in architecture and geology [Zeh06], or even surgical planning in medicine [DGBW09, YKD\*11].

Being a three-dimensional (3D) tensor field in nature, stress field is not straightforward to be visualized with existing virtual de-

sign systems. As a compromise, designers usually compute the von Mises stress or the maximum principal stress from the stress tensor, and then display them as color-coded scalar fields. This substitution is not intuitive for the user to perceive the stress. First, volumetric data visualization techniques are still required to show the 3D scalar field, and users have to adjust the cutting plane or parameters of transfer functions to observe the data inside the object. Second, the 3D stress tensor is tailored to a scalar, which inevitably loses the information of the varying traction related to different orientation. Different 3D tensor visualizations have also been proposed by the researchers [DH93, ZHT07, GRT17]. While the tensor glyphs or streamlines are proven to be effective to understand the tensor

fields, they are still not intuitive for novice users to understand the stress field. Stress field varies with different loads or constraints specified on the object, which are often adjusted and altered during the design process in order to examine the stress of the model under different configurations. In these cases, the design mode, simulation mode, and visualization mode are switched frequently, which complicates the interaction process.

Motivated by the recent success of virtual reality techniques which enhances the human’s senses for various expensive tasks in the physical world [KCT\*17, AGT\*15], we propose a virtual reality system for navigating the stress distribution inside objects in this work, as illustrated in Fig. 1. In order to intuitively convey the stress information to the user, we design and develop a wearable haptic interface, which maps an interior stress tensor inside the object to the haptics forces rendering along the finger under different navigation configurations. Conventional haptical interfaces are usually adopted to display contact, softness, friction or surface geometry and texture. To the best of our knowledge, no previous study has been raised to use haptics to render volumetric stress tensor field. In addition, we also use optical sensors to locate the user’s fingertips in real time, which is synchronized with the stress navigation. In combination with a wearable haptical device, the rendered stress tensors are finally exerted on the fingertips, which helps the user to perceive the 3D stress field interactively and intuitively. With the help of this system, we design several interaction modes for the task of 3D stress field navigation and conduct experiments to verify the efficiency of our system.

In the rest part of the paper, after a summary of related work in Sec. 2, we introduce our system setups in Sec. 3 including the detailed hardware and software settings. We experiment our system with two designed interaction modes and evaluate our design in Sec. 4. Finally, we discuss and conclude our work in Sec. 5.

## 2. Related Work

**Display of Stress Field.** As a second-order tensor field, traditional way to display stress inside an object to end user is to use the visual channel. Various visualization techniques such as glyphs [GRT17], streamlines [DH93] or image/texture-based methods [ZHT07] are introduced to present symmetric tensor fields. These basic techniques are also combined to visualize general tensor fields [PLC\*11]. In the case of displaying 3D tensor field inside an object, volume rendering techniques are also required to map the volumetric data onto the screen space [BW03, KWH00, Zeh06] or with the CAVE-based VR display [LSSB12]. As pointed out in [HHK\*14], a technique which is intuitive to the domain-specific users is highly preferred in tensor field visualization. Although it is practical to render stress tensor fields using visualization techniques for general tensor fields, we opt to display stress tensor fields using a haptical interface, for an intuitive perception of the force-related data encoded in a stress field.

**Haptical Interfaces for Engineering Applications.** Haptical interfaces are traditionally introduced to reproduce the perception of touching or grasping objects. Researchers developed various algorithms to render the forces in the manipulation of rigid or soft objects [SCB04, SH17]. Avila and Sobierajski proposed to use haptical interface to perceive volume data and opacity transfer functions

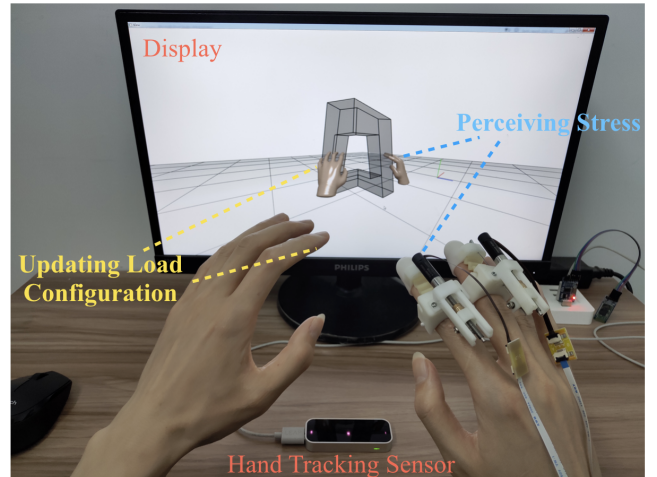


Figure 2: The proposed bimanual user interface .

are used to display volumetric scalar fields [AS96]. Instead, we focus on stress tensor field for engineering applications in this work.

As force-related feedbacks are common in product design, haptical interfaces have been developed in engineering applications [Xia16]. Generally, haptical information includes force, torque, and tactile feedbacks. In this work, we focus on the force feedbacks because we intend to explore stress fields in design. In previous works, force feedbacks are shown to be effective in virtual shape modeling using desktop devices [FOS\*08] or virtual assembly using robot arms [SWH\*12].

In order to better democratize haptics, wearable devices are also invented and used in various applications, such as pneumatic feedback actuators for virtual palpation [LLN\*14], cutaneous devices based on servomotors [PSH\*16], and electrostatic clutches [HVSH18] for virtual grasping. An advantage of these lightweight wearable haptical devices is that hand gestures can be tracked using off-the-shelf optical sensors such as leap motion. In parallel with the development of hardware, researchers are also improving the modeling of virtual hand models [JF11, HT16] as well as their interaction with deformable objects [MSB\*04].

Our work is also inspired by virtual reality systems which enhance the sensing of human beings. For example, with a comprehensive simulation, virtual reality techniques allow human beings to sense the environment with adjusted gravity [KCT\*17] or experience with an elongated arms [AGT\*15]. In this work, we adopt virtual reality techniques to allow users to directly “feel” the stress distribution inside an object by probing their hands into the model, which is not possible in the real physical world compared with other interactions like as touch or grasp.

## 3. System Setup

### 3.1. System Overview

We show the user interface in Fig. 2 with the corresponding system diagram in Fig. 3. The goal of our system is to help users

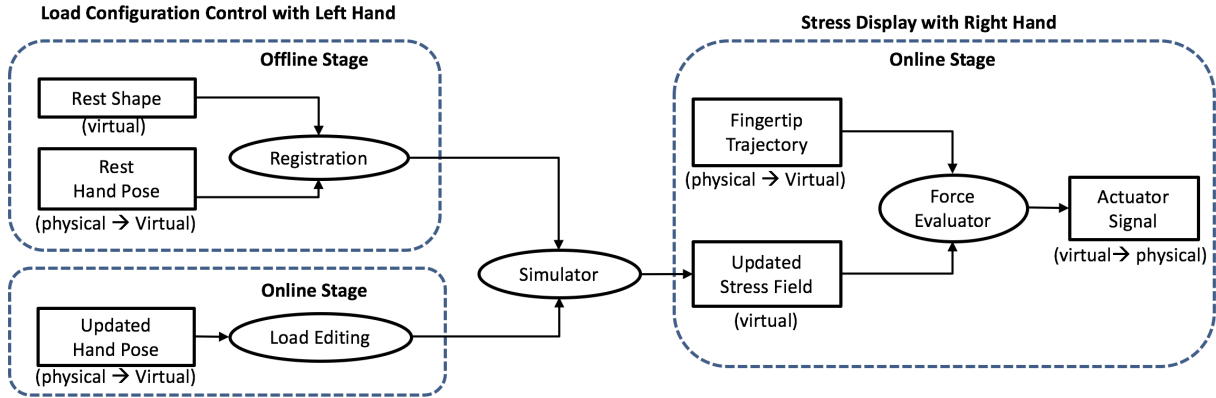


Figure 3: The system diagram.

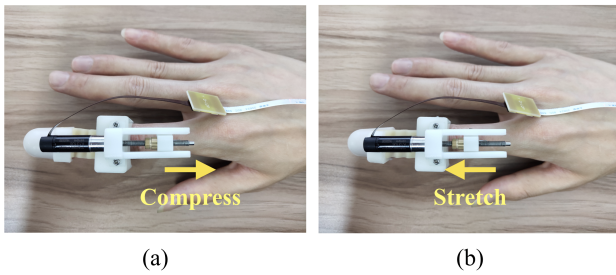


Figure 4: The proposed cutaneous device provides haptical feedbacks by compressing or stretching the finger skin.

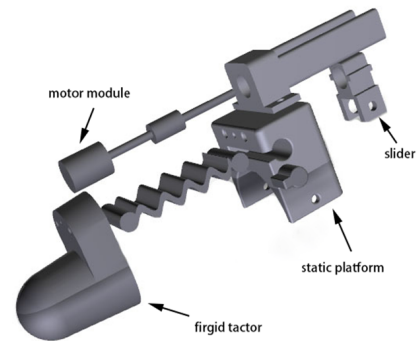


Figure 5: The exploded view of the haptic device.

explore the stress distribution of a designed 3D model. We start with a given 3D model. In order to evaluate whether this model is structurally sound in various situations, a user will need to examine the stress distribution inside the object under different prescribed load configurations. There are two types of interactions integrated in our system: the stress field manipulation by prescribing specific load configurations (Sec. 3.3) and the stress exploration by probing inside the object's volume (Sec. ??). To implement the system, we use a Leap Motion controller [WBRF13] to locate the position of the hand joints and fingertips. The Leap Motion uses two monochromatic IR cameras and three infrared LEDs to track the hand in 3D space. It observes a hemispherical area up to a distance of 1 m with an accuracy up to 0.01 mm. For the force feedbacks, we develop a small wearable fingertip haptic device (Sec. 3.2), which is lightweight and compatible with the optical hand tracker in our system.

### 3.2. Wearable Fingertip Haptic Device

We show in the Fig. 4 a prototype of the wearable fingertip haptic device and its exploded view in the Fig. 5. The device is designed to move a rigid tactor in contact with the fingertip providing forced sensations. In our application, we prefer a device which is wearable, lightweight and compatible with Leap Motion controller. With this consideration, we place the fingertip haptic device

on the back of the finger. As shown in Fig. 5, the device is composed of four parts, a static platform with soft adhesive connector, a motor module, a slider, and a spherical tactor. The static platform houses a motor module of small size and connects the tactor with the soft adhesive connector. The slider is mounted at the spindle drive and linked the rigid tactor by a cable. The motion of the slider is constrained by trails on the frame of the static platform. The tactor contacts with the finger pad providing tactile cues. The static platform is made of 3D-printed ABS and grips both sides of the finger. The device weighs 34.6 g and its size is approximately of 125 mm × 28 mm × 38 mm.

Human can perceive a realistic enforced sensation because of the skin deformation [SMMR98]. The motor module controls the motion of the slider, which moves the tactor toward the fingertip. The working principle of the device is depicted in Fig. 4. When the motor rotates in the clockwise direction, the slider will slide up to strengthen the tension of the cable, the tactor applies an enhanced force to the finger. On the other hand, when the motor rotates in the counter-clockwise direction, the slider will slide down to weaken the tension of the cable, the tactor applies a weakened directional force to the finger. The shape of tactor is designed to fit the fingertip, and it has a motion workspace of +9 mm. The magnitude of the tactor's motion can be varied based on the desired tactile cues.

The adopted motor module consists of a DC motor (maxon 347724), an encoder, and spindle drive. The maximum feed force continuously applied to stretch the skin is  $4 N$ . The motor module is controlled by an electrical hardware that consists of a microcontroller (STMicroelectronics, STM32F103CBT6), a motor driver (Texas Instruments Inc., DRV8830), a step-down converter (Texas Instruments Inc., TPS62046) and a boost converter (Texas Instruments Inc., TPS61092). The microcontroller communicates with a PC via a serial port. The device is powered by one battery (3.6 V 1000 mAh, LIB).

**Differential Threshold** An important preliminary experiment is performed to determine how to correctly modulate the cutaneous stimuli to be provided. This test evaluates the differential thresholds for the user to discriminate the tactile cues. The definition of differential threshold in Psychophysics was “the smallest amount of stimulus energy necessary to produce a just noticeable difference (JND) in the sensation” [Ges13], which is a relatively subjective measure. It indicates how much difference two stimuli need to have in order to be noticed and felt as different by a user. The differential threshold (i.e. JND) of a perceptual stimulus follows the fact that people are usually more sensitive to changes in weak stimuli than similar changes in stronger stimuli and this fact was studied by the physician Ernst Heinrich Weber. According to the *Weber’s law*, the relationship between JND and reference stimulus is  $JND = kI$ , revealing that the differential threshold JND increases with the increasing stimulus intensity  $I$ , and the linear proportional constant  $k$  is referred to as Weber’s fraction.

We designed an experiment to obtain the JND of our device. 12 participants (mean age 23, 10 males and 2 females) performed the experiment. 10 of them had previous experience with haptic interfaces. None of the participants reported any deficiencies in their haptic perception ability, and all of them were right-hand dominant. Subjects were required to wear the device on their right index finger, as shown in Fig. 4. Subjects wore noise canceling headphones playing white noise to minimize environmental distractions and cancel out noise from the DC motor.

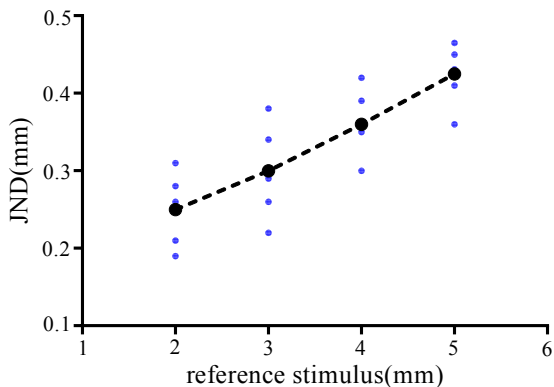


**Figure 6:** The JND of the wearable haptic device.

The simple up-down method [Lev71] was used to evaluate the differential threshold for the user to discriminate the tactile cues.

We considered the task completed when six reversals occurred. Subjects wear the developed cutaneous device and tell the experimenter when the two stimuli provided are felt different. We used a step-size for the motor module of  $r = 1$ , that corresponds to a normal displacement of the slider of  $0.5 mm$ . We test the JND at four standard stimuli:  $2 mm$ ,  $3 mm$ ,  $4 mm$ , and  $5 mm$  of displacement into the finger pad. Each participant performed 6 trials of the simple up-down procedure, with two repetitions for each standard stimulus considered. Fig. 6 shows the differential thresholds registered for each reference stimulus. For the reference stimuli of  $2 mm$ ,  $3 mm$ ,  $4 mm$ , and  $5 mm$ , the average JNDs are  $0.25 mm$ ,  $0.3 mm$ ,  $0.36 mm$ , and  $0.425 mm$ , respectively. Thus, the Weber fractions are  $0.125$ ,  $0.1$ ,  $0.09$ ,  $0.085$  following Weber’s Law. We use the least square method to fit the Weber fraction for the device and the estimated  $k = 0.092$ .

In our design, the wearable haptic device could provide a displacement ranging to  $\pm 9 mm$  for an index finger of an adult, corresponding to a maximum JND of  $0.828 mm$ . Considering the maximum stimuli of  $9 mm$  and a step of minimum displacement of the slider  $0.5 mm$ , the wearable device is able to provide around 30 discriminable levels of stimuli. In other words, the perceptual resolution of the device reaches about  $1/30$  of the range. As the system runs at a frequency of  $30Hz$ , it is sufficient to provide the feedbacks during the interaction.

### 3.3. Controlling the Load Configuration

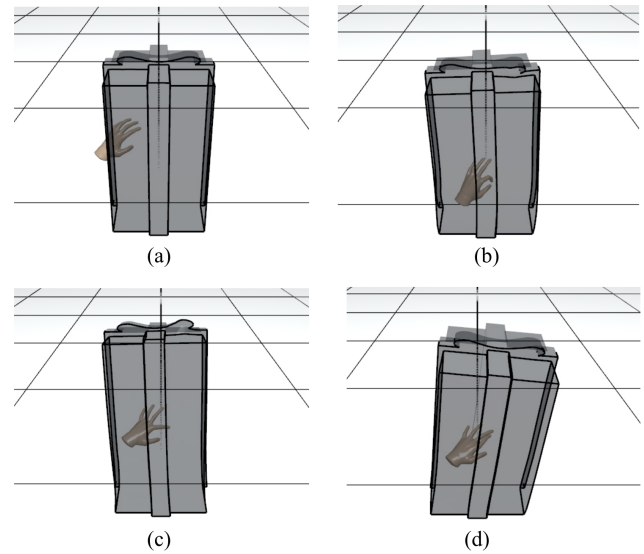


**Figure 7:** We edit the load configuration on the designed shape by immerse the left hand of the user into the object (a) and interactively update the stress field under the various poses of the hand (b,c,d).

As shown in the Fig. 7 (left), we start from a pre-designed shape and navigate the stress distribution after editing its load configurations in this mode. We virtually locate the hand into the 3D model as if a skeleton embedded in the model and exert external forces on

the fingertips and joints by tracking their positions. The interaction of this mode includes a registration step and a load editing step.

In the registration step, we first tetrahedronize the 3D model and normalize it to have comparable scales of the tracking hand. Specifically, we keep the bounding box of the model of twice size of the hand. We suppose that the 3D model is represented as a tetrahedral mesh  $(V, T)$  with a list of vertices  $V = \{v_1, v_2, \dots\}$  and a list of tetrahedrons  $T = \{t_1, t_2, \dots\}$  where  $t_i$  contains the indices of the vertices on the  $i$ th tetrahedron. After the 3D model is loaded, user adjust the gesture of his or her hands to find a appropriate initial position of the hand, which is denoted by a list of points  $\{\bar{\mathbf{p}}_1, \bar{\mathbf{p}}_2, \dots\}$  including the position of fingertips, joints and other key samples on the hand skeleton. We then check whether any of the key points are inside the 3D model. If the  $i$ -th key point  $\bar{\mathbf{p}}_i$  is inside the model, we find the tetrahedron which it locates in and mark it as an *active key point*. It is used to control the load distribution in the mode. After the user is satisfied with the initial embedding of his or her hand, the system stores the barycentric coordinates  $\{\omega_{ij}\}_{j=1}^4$  of each active key point  $i$  which is inside the  $l$ -th tetrahedron, such that  $\bar{\mathbf{p}}_i = \sum_{j=1}^4 \omega_{ij} \mathbf{v}_{lij}$ . We also precompute the stiffness matrix  $K$  of the 3D model, which will be used to compute the stress distribution in the load editing step.

In the load editing step, the user is allowed to change the hand gesture to control the load configuration. Suppose the updated position of the  $i$ -th active key point is  $\mathbf{p}_i$ , we define the load on the  $i$ th point as  $\mathbf{f}_i = w(\mathbf{p}_i - \bar{\mathbf{p}}_i)$ , where the weight  $w$  controls the magnitude of the load and is set according to different applications. We then use finite element method (FEM) to compute the stress distribution inside the 3D model. As in the FEM model, the forces are defined on the FEM nodes, we therefore distribution the force onto the vertices according to the pre-stored barycentric coordinates  $\mathbf{f}_{lij} = \omega_{ij} \mathbf{f}_i$ . Under the given external forces, we use standard FEM method to compute the deformation  $\mathbf{u}$  of the model by solving  $K\mathbf{u} = \mathbf{f}$ . In most structural analysis applications, only small-scale deformation is involved. Therefore, we just implemented the linear elasticity with constant  $K$ . For nonlinear elasticities,  $K$  also depends on the current deformation (i.e.  $K = K(\mathbf{u})$ ), and one needs to use nonlinear solvers like Newton's method to iteratively find the corresponding model deformation. After the deformation is obtained, we update the strain tensor of each element and compute the stress tensor according to pre-specified material properties of the 3D model. We refer the reader to [SB12] for a detailed description of the FEM formulation.

## 4. Evaluation

With help of the developed system, users can interactively perceive the 3D stress field inside an object with up to 10,000 vertices and 40,000 tetrahedrons. The proposed system supports both interactive adjustment and navigation of the stress field. We evaluate our system by two experiments. First, we verify the effectiveness of the single finger interaction in perceiving the stress. Then, we validate the our system in an engineering application.

### 4.1. Single Finger Interaction

We conducted one experiment to assess the effectiveness of the user experience during feeling the stress distribution inside an object using the haptic device. We first tested our device and system by using a single finger, in comparison with the interaction by using visual channel. The same group of 12 participants (mean age = 24, 10 males and 2 females) that participated in the JND test were involved in this experiment. Similarly, subjects wore noise canceling headphones playing white noise to minimize environmental distractions and cancel out noise from the DC motor.

The experiment setup consists of a virtual environment, the proposed haptical feedback device, and a Leap Motion. A participant sits in front of a computer screen wearing the tactile feedback device on the right index finger. The Leap Motion controller is used to track the position of the finger. The virtual environment was rendered in C/C++ using OpenGL.

#### 4.1.1. Method

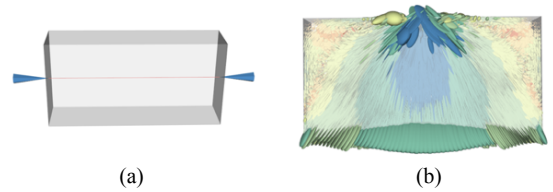


**Figure 8:** In the user study we use (a) a cuboid domain of the stress field and the red line connecting the left center and right center points (pointed by the blue arrow) as the navigation path. (b) One example of the stress field visualized by using ellipsoid glyphs for the user study.

In this experiment, our hypothesis was that users could tell the spatial variation of the directional stress and find the location with extreme stress from the haptical feedbacks by using a single finger. We also provided a typical glyph-based visualization of the same stress distribution, in order to study whether the haptical feedbacks from our system enabled a similar or better perception of the stress distribution in comparison with visual cues. For a better control of the study, we imported a stress tensor field defined in a box domain at once and asked the participants to report the distribution of the directional stress along a horizontal line between the center of the left face and the right face, as illustrated in Fig. 8(a). Different stress fields were displayed to the participants in a reference mode and a comparison mode.

In this experimental mode, no visual cues were given to indicate the change of stress field. Subjects were instructed to wear the tactile feedback device on the right index finger and were also given explanation of the haptic scenario which was rendered to them. The hand motion was tracked by the Leap Motion controller and projected to make the right index finger on the center line. In order to increase the illusion of telepresence, a virtual human hand mimicked the participant's hand pose in the virtual environment. When the index fingertip was moving inside the domain, the wearable cutaneous device provided an amount of displacement corresponding to the directional stress to the participant's finger, providing

them with the compelling sensation of feeling the quantity of the stress tensors. Participants were asked to point out which cells had maximum-and-minimum directional stress during their interaction. We recorded the location where they reported an extreme force and timed the exploration during the user study.

In the comparison mode, no cutaneous feedback was provided. We use a glyph-based visualization to display the stress field, where the typical ellipsoid glyph is used in the study [cF65]. Subjects were given explanation of the ellipsoid glyphs, in which the size of each ellipsoid corresponds to the eigenvalues of the stress tensor and the orientation encodes its eigenvectors. In addition, the glyph is set by color-mapping the surface of the ellipsoid based on the von Mises stress value  $\sigma_{vm}^2 = ((\Delta\sigma_{1,2})^2 + (\Delta\sigma_{2,3})^2 + (\Delta\sigma_{3,1})^2 + 6(\sigma_{12}^2 + \sigma_{23}^2 + \sigma_{31}^2))/2$  where  $\Delta\sigma_{i,j} = \sigma_{ii} - \sigma_{jj}$  and  $\sigma_{ii}$  is the  $i, j$ th element of the stress tensor  $\sigma$ . The warmer(e.g. red) colors or lighter shades represent higher stresses(compressing is positive) and the cooler(e.g. blue) colors or darker shades indicate lower stresses. We implemented the visualization using the tools provided by VTK [SML06]. One example of the visualization is shown in Fig. 8(b). Subjects were required to observe the ellipsoid glyph and asked where the extreme directional stress was located along the testing path.

#### 4.1.2. Results and Discussion

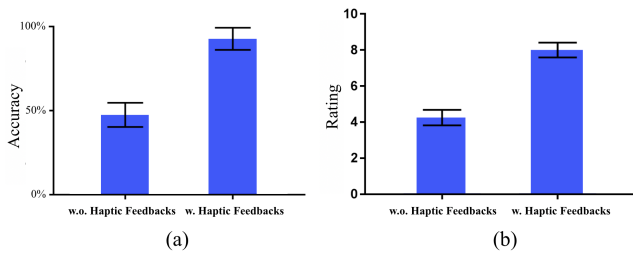


**Figure 9:** The results of the user study of single finger interaction. (a) The ratio that users correctly point out the trend of the varying stress along the center line is higher with our haptic feedbacks. (b) The user rating about the efficiency of the single point interaction using our device in comparison with using visual cues is higher.

We showed the results of the user study in Fig. 9. Each participant successfully completed the task by using our haptical interface, and the average time for finding the extreme directional stress is about 53.47seconds. We computed the distance between the reported location of each subject and the exact location of the extreme directional stress as the measurement of accuracy. The average error of the point is about 6% of the box length. The results in Fig. 9(a) showed that the proposed interface was effective in perceiving the stress distribution. In comparison, because of the occlusion in the visualization, the subjects usually could not correctly point out the extreme locations from the visual cues only. A complex interaction through the visualization was often required by the subjects in the task.

## 4.2. Application in Engineering Design

After we verified the effectiveness of the haptical interface in perceiving stress distribution inside a 3D domain, we continued to evaluate our system with an engineering application. In this experiment, our hypothesis is that our system is useful for engineering applications such as examining and validating the strength of geometric design. We took an architecture model as shown in Fig. 2 to test our system.

### 4.2.1. Method

7 participants(mean age = 24, 5 male) performed the experiment. All of them were right-hand dominant, and gave informed consent. None of the participants reported any deficiencies in their visual or haptic perception abilities. Subjects wore noise canceling headphones playing white noise to minimize environmental distractions and cancel out noise from the DC motor. All the participants had background in engineering mechanics and experiences in industrial design. Two of them had experiences in using virtual reality systems.

The experiment setup was similar to the earlier experiment, except that in this experiment we provided two wearable devices on two fingers of each participant. The participants could perceive the computed stress on two fingertips simultaneously during the interaction. In the setup, we put the devices on the right hand and enabled the left hand to control the deformation of the model, as described in Sec. 3.3. In this case, the subjects were able to examine the stress distribution of the model under varying load configurations in one section, as demonstrated in Fig. ??(c).

In this application, we kept the vertices on the bottom of the model constrained as one boundary condition and use linear elasticity to model the stress field under different loads, as an architecture model was checked in this experiment.

With the above setup, subjects were first given a 10-minute section of introduction of the interface and 3-minute section to freely explore the system. Then each of them was first asked to move the right hand inside model which was deformed by the left hand. We asked them if they could tell the difference of the forces between the two fingertips. Each of them was randomly stopped to answer which finger was taken a larger force for a few times and we also recorded the directional stress rendered to the two fingers at that time. If they could not tell the difference, they could report no difference. After the experiment, we computed the ratio of the right answers, which was used to quantify if bi-finger interaction was helpful to perceive the spatial difference at the same time.

After the elementary test of the bi-finger interaction, we proceeded to a complex task. The participants were asked to check the weakest part of the model by changing the deformation configurations and exploring the stress distribution by moving the fingers in a real-world space. We recorded the spots where they stopped as the weak part of the design, as well as the time used in the interaction. We also had them rate their preference to our system and interviewed them after the experiment.

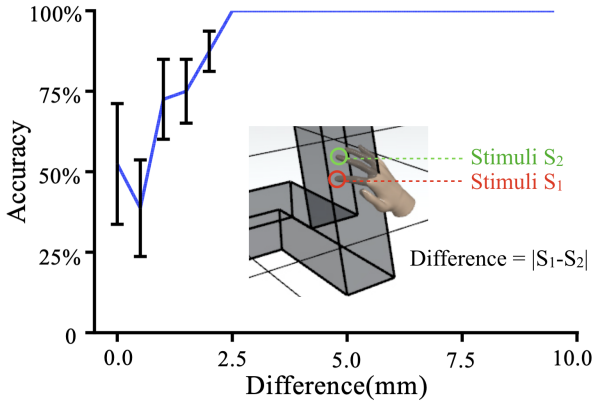


**Figure 10:** The experimental results of the bi-finger interactions. The ratio of the correct comparisons of the forces is high when the difference of the forces reaches 4 displacement units.

#### 4.2.2. Results and Discussion

We have collected 54 trials in the elementary test of the bi-finger interaction and plotted in Fig. 10 the ratios of the correct answers, which was referred as accuracy here. As we randomly created the trials, the overall accuracy was 86.5% in this experiment. Because larger difference of the rendered forces lead to easy perception in the comparison, we further studied how the accuracy varied with the difference of the rendered forces. As we eventually unified the force and converted it to the displacement of the slider, we use the unit of the displacement of the slider to describe the difference of the rendered force. As shown in Fig. 10, when there was no difference of the forces, users were able to tell that the two fingertips had the same stimuli with the probability around 60%. The accuracy was the lowest (around 50%) when the unit of the difference was 1. When the difference of the unit went to 4, users could always correctly tell which finger had a larger force. As we provided 200 units of difference in our hardware setting, users could distinguish the force applied on the two fingers in most times. In this case, they were fed with more information in complex tasks.

We then reported the behavior of our system in the complex task of finding the weak regions of the model, including the structurally weak region on the boundary and the cracks inside the model. Before we evaluated the proposed interface, we offline computed the weak regions of the model. We randomly applied varying loads on the model for two million times and found the vertex with the maximum von mises stress under each load configuration. If a vertex on the model was chosen as the weakest vertex for a large amount of times, we regarded it as a weak vertex. We grouped neighboring weak vertices to form weak regions and highlighted ten weakest regions of the model in Fig. 11. In the figure, we color-coded the frequency of the region which was chosen as the weakest under a specific load configuration and the red color represented that the region was more likely to break under a random load configuration.

In the complex task, having the goal of finding the weak regions in mind, users were asked to freely play with our system. They then reported the weak region if they found it always with a larger

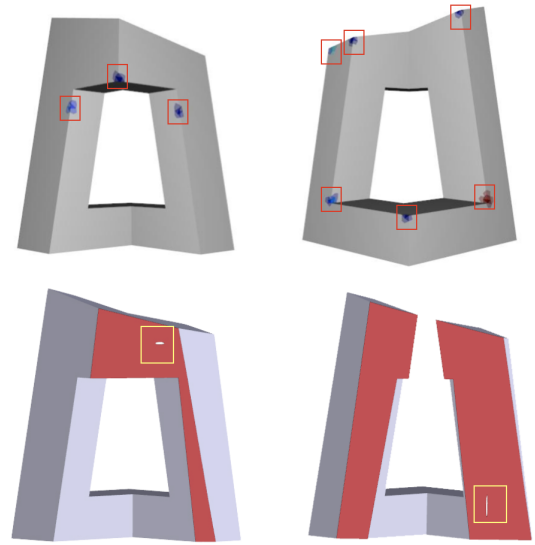


**Figure 11:** The weak regions used in the user study, including two cracks inside the model are to be detected.

directional stress in the exploration. If the position of the specified fingertip was close to the weak region (less the 5% of the diagonal length of the bounding box), we regarded a correct spot. Once a participant correctly found a weak region, we stopped the timing. For all the participants, it took around 3 minutes to complete the task, ranging from 1.75 minutes to 3.5 minutes. As reported by an architect, it usually took at least one hour for the same task by using traditional systems, because they had to manually design different load configurations and examine the volumetric model, which was time-consuming.

We also qualitatively studied the proposed system. Based on the transcripts, statement given by the participants were extracted. Similar statement were grouped to identify common feedback given by multiple participants.

Most of the participants found it easy to understand the interaction, comparing with the interaction using only the visual channel. They felt the interaction natural and it directly gave them force-related feedbacks in the complex task. They claimed that the occlusion in the volumetric data was disturbing, while moving their hands into the model was very convenient for them to perceive the stress field. During the interaction, the participant also found that it was necessary to provide them the visual cues about whether their hand was inside the model. Because the physical space for the hands are relatively large than the virtual space inside the 3D model, they would be more engaged in the task once they know their virtual hands were inside the 3D model.

The participants generally found it fun to play with the wearable haptical device. They could clearly feel the forces exerted on their fingertips and the device was sensitive in the interaction. A few of the participants preferred a less sensitive feedbacks, as they would sometimes stop to feel the forces, while their hands were actually not perfectly stopped in the interaction and the feedback was fre-

quently changing. To this end, we could filter the noises in the hand motion to improve the interaction.

Other suggestions were about the hardware design. A few participants felt too much finger pressure in the extreme case. It could be alleviated by personalize the structural design of the device to improve the affordance to specific users. The participant who took the longest time to complete the task said that the system could be further improved by reducing the weight of the device, which was beneficial for long-term interactions.

## 5. Conclusion

We propose a system which helps users to perceive the stress field inside a 3D object. A wearable haptical device is introduced and a bimanual interaction is designed for the task. With the designed system, we enable the users to explore the stress field while controlling the load configuration on the given model. It is shown to be beneficial for applications in engineering design.

In the future, we will improve the hardware design for better accommodate the users in the task. A device providing both forces and torques would also make the interaction more flexible in perceiving a stress field. In this work, we focus on display the directional stress to the users. It is also an interesting topic to design a system to help finding topological structure of the stress field, such as degenerated points and separatrixes. It is also possible to improve our system by developing an immersive environment using a see-through near-eye display. We will study how to leverage the information from visual and haptical channel to further improve the efficiency in understanding stress fields.

## References

- [AGT\*15] ACHIBET M., GIRARD A., TALVAS A., MARCHAL M., LŠCUYER A.: Elastic-arm: Human-scale passive haptic feedback for augmenting interaction and perception in virtual environments. In *2015 IEEE Virtual Reality (VR)* (2015), pp. 63–68. 2
- [AS96] AVILA R. S., SOBIERAJSKI L. M.: A haptic interaction method for volume visualization. In *Visualization '96. Proceedings.* (1996), pp. 197–204. 2
- [BW03] BHALERAO A., WESTIN C.-F.: Tensor splats: Visualising tensor fields by texture mapped volume rendering. In *Medical Image Computing and Computer-Assisted Intervention - MICCAI 2003* (Berlin, Heidelberg, 2003), Springer Berlin Heidelberg, pp. 294–302. 2
- [cF65] CHENG FUNG Y.: *Foundations of Solid Mechanics*. Prentice-Hall, 1965. 6
- [DGBW09] DICK C., GEORGII J., BURGKART R., WESTERMANN R.: Stress tensor field visualization for implant planning in orthopedics. *IEEE Transactions on Visualization and Computer Graphics* 15, 6 (2009), 1399–1406. 1
- [DH93] DELMARCELLE T., HESSELINK L.: Visualizing second-order tensor fields with hyperstreamlines. *IEEE Computer Graphics and Applications* 13, 4 (1993), 25–33. 1, 2
- [FOS\*08] FAETH A., OREN M., SHELLER J., GODINEZ S., HARDING C.: Cutting, deforming and painting of 3d meshes in a two handed viso-haptic vr system. In *2008 IEEE Virtual Reality Conference* (2008), pp. 213–216. 2
- [Ges13] GESCHIEDER G. A.: *Psychophysics: the fundamentals*. Psychology Press, 2013. 4
- [GRT17] GERRITS T., RÖSSL C., THEISEL H.: Glyphs for general second-order 2d and 3d tensors. *IEEE Transactions on Visualization and Computer Graphics* 23, 1 (2017), 980–989. 1, 2
- [HHK\*14] HLAWITSCHKA M., HOTZ I., KRATZ A., MARAI G. E., MORENO R., SCHEUERMANN G., STOMMEL M., WIEBEL A., ZHANG E.: Top challenges in the visualization of engineering tensor fields, 2014. 2
- [HT16] HIROTA K., TAGAWA K.: Interaction with virtual object using deformable hand. In *2016 IEEE Virtual Reality (VR)* (2016), pp. 49–56. 2
- [HVSH18] HINCHEM R., VECHEV V., SHEA H., HILLIGES O.: Dextres: Wearable haptic feedback for grasping in vr via a thin form-factor electrostatic brake. In *Proceedings of the 31st Annual ACM Symposium on User Interface Software and Technology* (2018), UIST '18, pp. 901–912. 2
- [JF11] JACOBS J., FROEHLICH B.: A soft hand model for physically-based manipulation of virtual objects. In *2011 IEEE Virtual Reality Conference* (2011), pp. 11–18. 2
- [KCT\*17] KIM M., CHO S., TRAN T. Q., KIM S. P., KWON O., HAN J.: Scaled jump in gravity-reduced virtual environments. *IEEE Transactions on Visualization and Computer Graphics* 23, 4 (2017), 1360–1368. 2
- [KSZ\*14] KRATZ A., SCHOENEICH M., ZOBEL V., BURGETH B., SCHEUERMANN G., HOTZ I., STOMMEL M.: Tensor visualization driven mechanical component design. In *2014 IEEE Pacific Visualization Symposium* (2014), pp. 145–152. 1
- [KWH00] KINDLMANN G., WEINSTEIN D., HART D.: Strategies for direct volume rendering of diffusion tensor fields. *IEEE Transactions on Visualization and Computer Graphics* 6, 2 (2000), 124–138. 2
- [Lev71] LEVITT H.: Transformed up-down methods in psychoacoustics. *The Journal of the Acoustical Society of America* 49, 2B (1971), 467–477. 4
- [LLN\*14] LI M., LUO S., NANAYAKKARA T., SENEVIRATNE L. D., DASGUPTA P., ALTHOEFFER K.: Multi-fingered haptic palpation using pneumatic feedback actuators. *Sensors and Actuators A: Physical* 218 (2014), 132 – 141. 2
- [LSSB12] LAHA B., SENSHARMA K., SCHIFFBAUER J. D., BOWMAN D. A.: Effects of immersion on visual analysis of volume data. *IEEE Transactions on Visualization and Computer Graphics* 18, 4 (2012), 597–606. 2
- [MSB\*04] MACIEL A., SARNI S., BUCHWALDER O., BOULIC R., THALMANN D.: Multi-Finger Haptic Rendering of Deformable Objects. In *Eurographics Workshop on Virtual Environments* (2004). 2
- [PLC\*11] PALKE D., LIN Z., CHEN G., YEH H., VINCENT P., LARAMEE R., ZHANG E.: Asymmetric tensor field visualization for surfaces. *IEEE Transactions on Visualization and Computer Graphics* 17, 12 (2011), 1979–1988. 2
- [PSH\*16] PACCHIEROTTI C., SALVIETTI G., HUSSAIN I., MELI L., PRATTICHIZZO D.: The hring: A wearable haptic device to avoid occlusions in hand tracking. In *2016 IEEE Haptics Symposium (HAPTICS)* (2016), pp. 134–139. 2
- [SB12] SIFAKIS E., BARBIC J.: Fem simulation of 3d deformable solids: A practitioner's guide to theory, discretization and model reduction. In *ACM SIGGRAPH 2012 Courses* (2012), pp. 20:1–20:50. 5
- [SCB04] SALISBURY K., CONTI F., BARBAGLI F.: Haptic rendering: introductory concepts. *IEEE Computer Graphics and Applications* 24, 2 (2004), 24–32. 2
- [SH17] SAGARDIA M., HULIN T.: Evaluation of a penalty and a constraint-based haptic rendering algorithm with different haptic interfaces and stiffness values. In *2017 IEEE Virtual Reality (VR)* (2017), pp. 64–73. 2
- [SML06] SCHROEDER W., MARTIN K., LORENSEN B.: *The Visualization Toolkit—An Object-Oriented Approach To 3D. Graphics*. Kitware, 2006. 6

- [SMMR98] SERINA E. R., MOCKENSTURM E., MOTE C., REMPEL D.: A structural model of the forced compression of the fingertip pulp. *Journal of Biomechanics* 31, 7 (1998), 639 – 646. [3](#)
- [SWH\*12] SAGARDIA M., WEBER B., HULIN T., HIRZINGER G., PREUSCHE C.: Evaluation of visual and force feedback in virtual assembly verifications. In *2012 IEEE Virtual Reality Workshops (VRW)* (2012), pp. 23–26. [2](#)
- [WBRF13] WEICHERT F., BACHMANN D., RUDAK B., FISSELER D.: Analysis of the accuracy and robustness of the leap motion controller. *Sensors* 13, 5 (2013), 6380–6393. [3](#)
- [Xia16] XIA P.: Haptics for product design and manufacturing simulation. *IEEE Transactions on Haptics* 9, 3 (2016), 358–375. [2](#)
- [YKD\*11] YANG Z., KOLLMANNBERGER S., DÜSTER A., RUESS M., GARCIA E. G., BURBKART R., RANK E.: Non-standard bone simulation: interactive numerical analysis by computational steering. *Computing and Visualization in Science* 14, 5 (2011), 207–216. [1](#)
- [Zeh06] ZEHNER B.: Interactive exploration of tensor fields in geosciences using volume rendering. *Computers & Geosciences* 32, 1 (2006), 73 – 84. [1](#), [2](#)
- [ZHT07] ZHANG E., HAYS J., TURK G.: Interactive tensor field design and visualization on surfaces. *IEEE Transactions on Visualization and Computer Graphics* 13, 1 (2007), 94–107. [1](#), [2](#)